Heat-Sealing Properties of Soy Protein Isolate/Poly(vinyl alcohol) Blend Films: Effect of the Heat-Sealing Temperature

Jun-Feng Su,[1,2] Xin-Yu Wang,[3] Zhen Huang,[2,3] Xiao-Yan Yuan,[1] Min Li,[3] Wen-Long Xia,[3] Cai-Ling Feng[3]

[1]*School of Material Science and Engineering, Tianjin University, Tianjin 300072, China*
[2]*Tianjin Key Laboratory of Refrigeration Technology, Tianjin University of Commerce, Tianjin 300134, China*
[3]*Institute of Materials Science and Chemical Engineering, Department of Packaging Engineering, Tianjin University of Commerce, Tianjin 300134, China*

Received 6 August 2008; accepted 19 July 2009
DOI 10.1002/app.31150
Published online 7 October 2009 in Wiley InterScience (www.interscience.wiley.com).

ABSTRACT: To promote the heat-sealing properties of soy protein isolate (SPI) films applied in the packaging field, we mixed a synthetic polymer of poly(vinyl alcohol) (PVA) with SPI to fabricate blend films by a solution-casting method in this study. To clarify the relationship between the heat-sealing properties and the heat-sealing temperature, strength, melting process, crystalline structure, and microstructure, variations of the heat-sealing parts of the films were evaluated by means of differential scanning calorimetry, tensile testing, scanning electron microscopy, X-ray diffraction, and Fourier transform infrared spectroscopy, respectively. The test results showed that both the PVA and glycerol contents greatly affected the melting behavior and heat of fusion of the SPI/PVA blends; these blend films had a higher melting temperature than the pure SPI films. The peel strength and tensile strength tests indicated that the long molecular chain of PVA had a main function of enhancing the mechanical properties above the melting temperature. With increasing heat-sealing temperature, all of the mechanical properties were affected by the microstructure of the interface between the laminated films including the chain entanglement, crystallization, and recrystallization. © 2009 Wiley Periodicals, Inc. J Appl Polym Sci 115: 1901–1911, 2010

Key words: biopolymers; blends; films; mechanical properties; structure-property relations

INTRODUCTION

Soy protein isolate (SPI) has gained increasing attention for the fabrication of biodegradable films, packaging films, and edible films as a potential substitute for existing petroleum-based polymers because of its low cost, easy availability, and complete biodegradability.[1–9] To date, physical, enzymatic, chemical, and physicochemical attempts have been made to modify the lower mechanical properties and higher moisture sensitivity of SPI films.[10–12] In addition to the previously mentioned two inherent characters that limit their application, sealing ability is another important property for these films in the making of packaging bags.[13] The ability to produce packaging film with such a sealing ability is now a major concern for SPI plastics and a key issue for their competitiveness for opening a new packaging material market.[14] However, no literature has reported on the sealing ability of natural SPI films. Therefore, it is very meaningful to investigate the heat-sealing ability of SPI-based films for packaging applications. At the same time, heat-sealing research results will provide valuable information about the structure and fabrication for natural protein materials and throw more light on SPI application.[15]

Compared to available sealing methods, including mechanical fastening, adhesive application, ultrasonic sealing, and high-frequency sealing, heat sealing is the most versatile method, with advantages of safety, convenience, good productivity, and high mechanical strength.[16] *Heat sealing* is defined as a process of joining two or more thermoplastic films or sheets by the heating of areas in contact with each other to a temperature at which fusion occurs; this is usually aided by pressure.[17] The heat-sealing property is normally evaluated mechanically by peel strength testing as determined by two aspects: the heat-sealing process and the microstructure of the heat-sealing part.[18] To enhance the sealing strength

Correspondence to: J.-F. Su (sujunfeng2000@yahoo.com.cn).

Contract grant sponsor: National Key Technology R&D Program of China; contract grant number: 2006BAD05A05.
Contract grant sponsor: Students Research Training of Tianjin University of Commerce; contract grant number: 2008038.

during the heat-sealing process, the pressure, temperature, and heat-sealing time are the three basic parameters to be considered.[19] The initial pressure makes an intimate squeeze between two films; then, the adhesion of two films is promoted by the action of heat from the outside with sufficient time. The peel strength of laminate films will distinctly be determined by the interface microstructure of the raw film materials after the heat-sealing process. It is well known that the mechanism of heat sealing is that the intimate contact of the sealing surfaces occurs after the molecular segment diffuse across the interface with entanglement.[17] Moreover, the cooling and recrystallization greatly affect the peel strength by chains diffusion and entanglement at the interfaces.[20]

A novel blend film of SPI/poly(vinyl alcohol) (PVA) compatibilized with glycerol fabricated by a solution-casting method was reported in our previous study.[21] Interestingly, it was proven that these SPI/PVA blend films with higher mechanical strengths had promising applications in the biodegradable packaging field.[22] With the importance of heat sealing for packaging films, the objective of this study was to evaluate the peel strength of SPI/PVA blend films with different PVA contents. Temperature was selected as the only parameter in the heat-sealing process with a stable pressure and heat-sealing time. In addition, the relationship between the heat-sealing temperature and the microstructure of the heat-sealing part was investigated by means of differential scanning calorimetry (DSC), X-ray diffraction (XRD), Fourier transform infrared (FTIR), and scanning electron microscopy (SEM).

EXPERIMENTAL

Materials

SPI powder (Type A©) with moisture content of less than 5.0% prepared under acid precipitation and containing more than 90% protein was provided by Harbin High-Technology Soy Protein Co., Ltd. (Harbin, China). PVA (molecular weight $\approx$ 9000) was purchased from SINPEC Shanghai Petrochemical Co., Ltd. (Shanghai, China). Analytical-grade glycerol (1,2,3-propane triol) with 95% purity was acquired from Tianjin Chemical Co. (Tianjin, China). Sodium hydroxide (NaOH) pellets were applied to prepare a 1.0-mol/L solution at room temperature in the laboratory.

Fabrication of the SPI/PVA blend films

The fabrication of the SPI/PVA blend films was described in a previous article with four steps.[21] First, an SPI water solution was prepared by the addition of 5.0 g of SPI powder into 100 g of deionized water; its pH value was adjusted from 6.8 to 10.0 by a 1.0-mol/L NaOH solution with continuous a 200-rpm stirring rate at 80°C for 60 min. The pH of the solution was monitored with an electronic pH meter (660 type, Lengpu Co., Shanghai, China). The raising the pH to 10.0 is well known to give a maximum protein unfolding and rearrangement state; a pH of 10 will bring high lysino–alanine linkage formation and high hydrolysis of asparagines and glutamine primary residues.[23]

Second, a PVA water solution (10 wt %) was stir-heated in a water bath maintained at 90°C for 90 min.

Third, a mixture including the prepared SPI solution, PVA solution, and glycerol was formed as the film-fabrication resin. The pH value of this film resin was again adjusted to 10.0 with a 1.0-mol/L NaOH solution at 80°C.

Fourth, the final prepared resin was vacuum-defoamed and poured onto a Teflon-coated metal sheet to form SPI/PVA films. We achieved a constant film thickness by casting the same amount of resin on one sheet in the same area. The Teflon-coated metal sheet was dried in an oven at 40°C for 6 h. These dried films were peeled off of the casting surface and were coded as P-0, P-10, P-15, P-20, P-25, and P-30 with the PVA weight ratios in the SPI/PVA blends controlled at 0, 10, 15, 20, 25, and 30%, respectively. Another series of SPI/PVA films with glycerol was fabricated with the same casting method and were coded as P-PVA-*n*, where *n* is the weight percentage of glycerol based on the SPI in the blend (wt %, glycerol/SPI).

Heat-sealing process

The heat-sealing process was carried out on a heat-sealing testing machine (HSG-C, Brugger, Muenchen Deuschland, Germany) with a pair of removable sealing jaws, whose heat-sealing temperature could be individually adjusted between ambient temperature and 300°C. Figure 1 shows the cross-sectional illustration of the sealing jaws and the laminate films placed between silicone rubbers. The temperature rose sharply toward the setting temperature with heat dispersion through the silicone rubbers. In this study, the heat-sealing temperature was kept at the peak temperature isothermally for 0.1 s with a 150-kPa pressure. At last, the heat-sealing films were removed from the jaws after they were cooled for 5.0 s. Because of the heat transfer lag in the polymer, the actual temperature inside the laminated films [polymer melting temperature (T_m)] did not rise up to the setting heat-sealing temperature during such a short sealing time.[17] The heat-sealing temperature was defined as the setting temperature recorded on the machine, which was equal to the temperature outside of the film surfaces.[24]

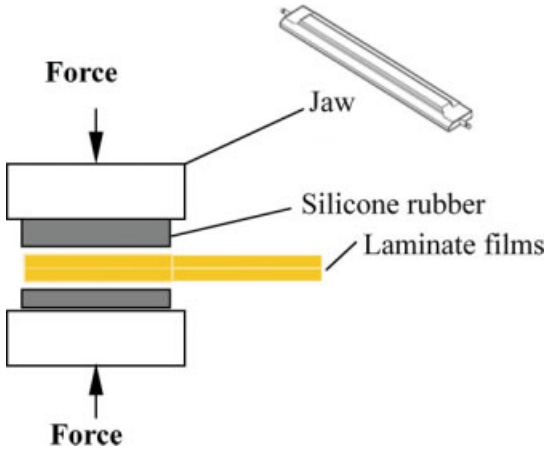

Figure 1 Cross-sectional illustration of the sealing jaws and the laminate films placed between silicone rubber. [Color figure can be viewed in the online issue, which is available at www.interscience.wiley.com.]

Peel strength tests

The peel strengths were measured by peel tests with a crosshead speed of 100 mm/min. Figure 2(a–c) illustrates the peel testing direction and sample (100 × 10 mm^2) dimensions with a heat-sealing area of 10 × 10 mm^2. To achieve the peel strength, a sample was gripped at the non-heat-sealed part and peeled open at 180°. The maximum load attained was used to calculated the peel strength (N/10 mm). The final peel strength was calculated from the average value of triplicate measurements for each type of film with individually prepared films. Three failure types occurred during the peel tests and were defined as separation between the two layers in contact [Fig. 2(d)], peeling by rupture of the lower cohesion layer [Fig. 2(e)], and tearing [Fig. 2(f)].[17]

Tensile tests

As the heat-sealing part usually exhibits a higher tensile strength than the gripped part in a film sample, a circular notch promotes the tensile deformation right in the middle of the heat-sealing zone.[25] Figure 3 illustrates a circular notch (radius = 5 mm) punched on the heat-sealing area of a film sample with a size of 15 mm (width) × 90 mm (length). To achieve uniform samples and notches, outlines were drown on the films according to a size of 90 × 15 mm^2, and notches were punched carefully before the samples were cut into strips. During the punching process, it was important that the perforator guide were aligned with the sample outlines to satisfy the accurate position of the circular notches. The machine direction (MD) and the transverse direction (TD) referred to the directions along the length and width of the heat-sealing samples.

DSC analysis

DSC curves were tested with a DSC TA2010 controlled by a TA5000 system (TA Instruments, New Castle, DE). Film samples (10 mg) were placed in hermetically sealed aluminum TA pans and heated at a speed of 5°C/min from 0 to 250°C. T_m was determined as the peak temperature of the endothermic event of a DSC curve, and heat of fusion (H_f) data were calculated from the melting area of a DSC curve automatically.

XRD tests

XRD patterns were measured with a powder diffractometer (Rigaku D/max 2500v/pc, Tokyo, Japan) to characterize the crystalline structure of the samples. According to a previous analysis,[21] the samples were scanned from 14 to 28° (2θ) at 5°/min with the application of 0.1542-nm Cu KαX-ray radiation.

FTIR analysis

The casting film samples were dried *in vacuo* at room temperature for 24 h and then cut into small

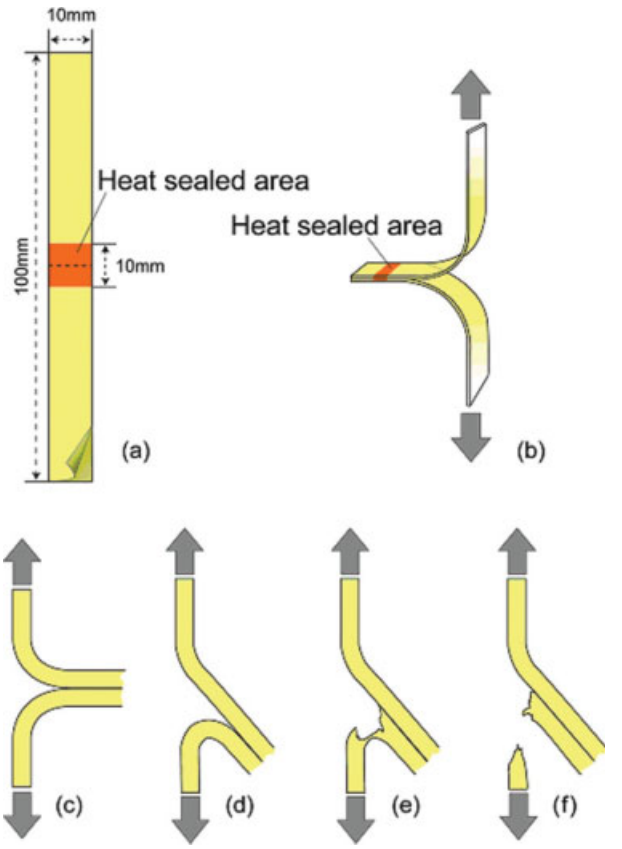

Figure 2 Illustration of the peel strength measurement of the heat-sealing samples: (a) sample dimensions, (b) peel testing direction and types of peel tests, (c) peeling, (d) peel separation, and (e,f) tearing failure. [Color figure can be viewed in the online issue, which is available at www.interscience.wiley.com.]

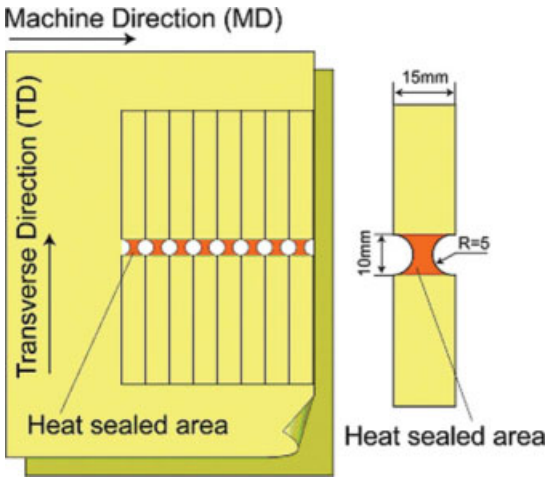

Figure 3 Illustration of tensile testing samples with circular punches (radius = 5 mm). [Color figure can be viewed in the online issue, which is available at www.interscience.wiley.com.]

pieces to be pelletized with KBr before the FTIR measurements. FTIR spectra were obtained on a Nicolet (Tokyo, Japan) Magna 750 spectrometer with a deuterated triglycine sulfate detector and Omnic 3.2 software with 128 scans at a resolution of 4.0 cm^{-1} in a range of wave numbers from 4000 to 400 cm^{-1}.

SEM morphology

The film samples were stuck by double-side electrically conductive carbon tape and then coated with thin gold layers about 200 Å thick. The SEM surface morphologies of the film samples were characterized (SEM XL30, Philips, Holland) at an acceleration of 5 kV.

RESULTS AND DISCUSSION

Melting characteristics of the SPI/PVA films tested by DSC

The heat-sealing temperature had to be equal to or higher than T_m; the laminated films were melted and sealed following with the chains entanglement across the interfaces.[17] As the heat-sealing time was very short (0.1 s), the degradation of natural SPI in the films could be omitted during heat softening. This means that T_m of the SPI/PVA blend was the minimum heat-sealing temperature for the polymeric films. Figure 4(a,b) shows the initial heating DSC curves (first run) of the pure SPI and PVA. Although SPI has been widely studied, the literature has reported no consistent results on the SPI glass-transition temperature and T_m because of the complex protein structure.[26] In this study, pure PVA had a T_m of 225°C; SPI melting occurred in a temperature range of 100–200°C with a very broad melting peak, and 145°C was determined as its T_m. All these melting characteristics accorded with reported results.[22] Before we determined T_m of the SPI/PVA blend, it was necessary to examine the compatibility of SPI and PVA to ensure that the blend was homogeneous in macroscopic level with a single T_m. Typical samples of P-10 and P-20 were selected to evaluate this problem.

Figure 4(c,d) shows that the SPI/PVA blend had good compatibility with only one melting peak. In addition, compared to P-20, P-10 had a broader T_m, ranging from 150 to 175°C. Similar articles reported that composites of PVA and natural polymers (including starch, cellulose, chitin, chitosan, wheat protein, egg protein, lignin, and sodium alginate) showed good biocompatibility.[27–31] The mechanism reported was that there were strong interactions and crystalline between PVA and natural molecules. Another phenomenon was that the addition of glycerol (only 1.0 wt % based on SPI) greatly affected the melting behaviors of the SPI/PVA blends, as shown in Figure 4(e,f). Both P-10-1 and P-20-1 had a decreased T_m with a broader T_m range compared to P-10 and P-20. The reason for this phenomenon was that glycerol could be inserted into the crystal structure and decrease the crystalline degree of polymers.[32,33]

Another conclusion could be drawn from the DSC curves: that PVA content was a main factor greatly affecting the melting process of the blends. Because the same heat pressure (150 kPa) and heat time (0.1 s) were adapted to simplify the heat-sealing process, H_f based on the heat-sealing temperature determined the ultimate heat-sealing results. Figure 5 shows the H_f data for samples P-5, P-10, P-15, P-20, P-25, and P-30 with/without glycerol, respectively. With increasing content of PVA in the blends, these samples needed more heat to make the long molecule melt. Meanwhile, the addition of glycerol decreased the value of H_f for the same sample. For example, value of H_f for P-5-1 (50.5 J/g) was less than that of P-5 (65.2 J/g). This result also proved the analyses in Figure 4 that show that the glycerol could destroy the crystalline microstructure and that the SPI/PVA/glycerol blend needed less heat to be converted to the melting state.

Effect of the heat-sealing temperature on the peel strength

In the peeling tests, fracture section could occur inside or outside the heat-sealing part, which was an indication of adhesion strength. These results supply information about the relationship between T_m and the surface molecular structure. Figure 6 shows the peel strength data of samples P-5, P-10, P-15, P-20, P-25, and P-30 without glycerol in a heat-sealing

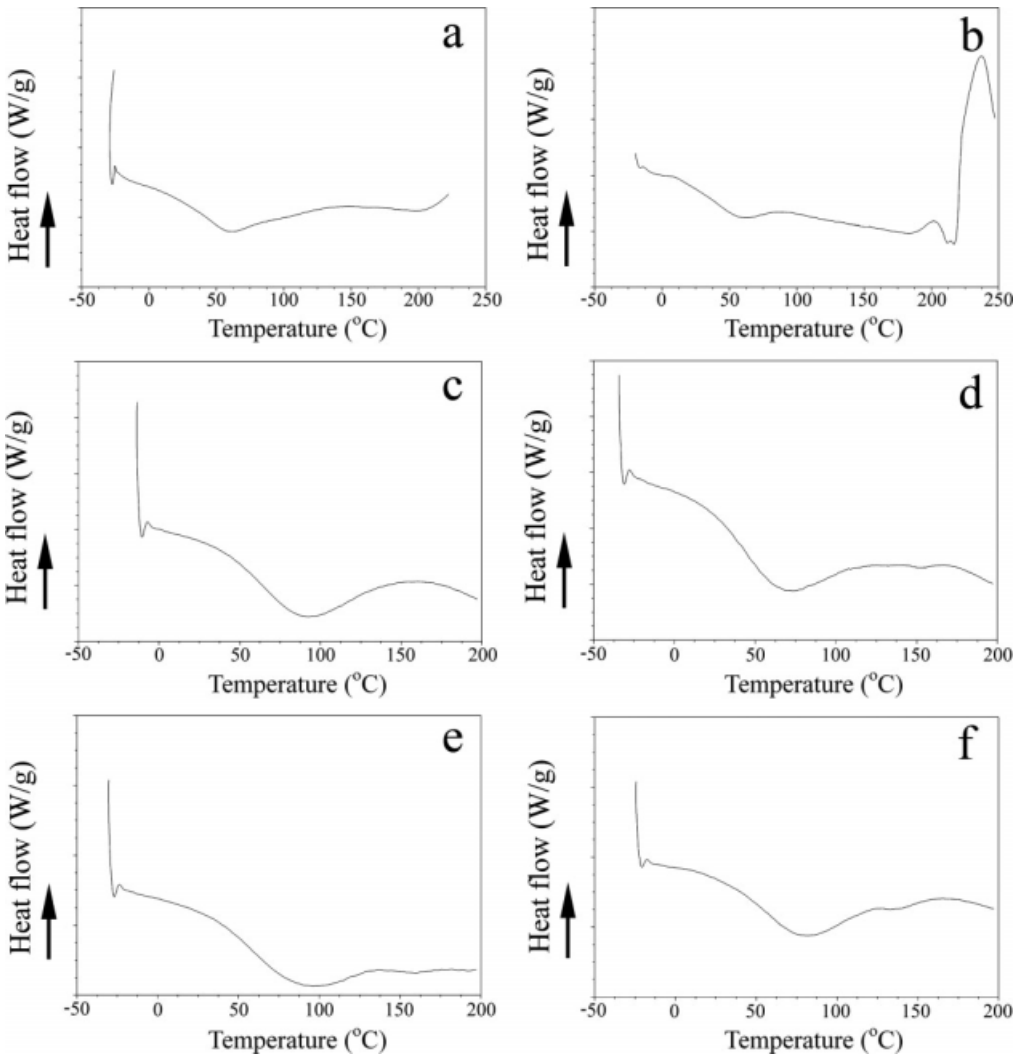

Figure 4 DSC curves of the blend films: (a) pure SPI, (b) pure PVA, (c) P-10, (d) P-10-1, (e) P-20, and (f) P-20-1.

temperature range of 170–250°C. When the heat-sealing temperature was lower than 170°C, all films were lead into a peeling separation without satisfying heat-sealing properties. This result accorded with the previous DSC analysis in that the blend did not melt under the lower temperature of 170°C. When the heat-sealing temperature increased higher than 180°C, the peel strength for all samples sharply increased. As the pure PVA had a higher T_m than SPI, a higher PVA content in the films brought a relatively higher heat-sealing temperature. However, the increasing ratios of peel strength were different, as shown by a comparison of the slopes of the temperature–healing strength curves. The peel strength for P-5 was in the range 6.4 MPa (170°C) to 6.8 MPa (250°C), whereas P-30 had peeling strengths from 7.1 MPa (170°C) to 21.0 MPa (250°C). P-30 had the maximum increasing ratio in the temperature range of 180–230°C. Interestingly, nearly each sample had three types of peeling processes (peeling separation, peeling, and tearing) with

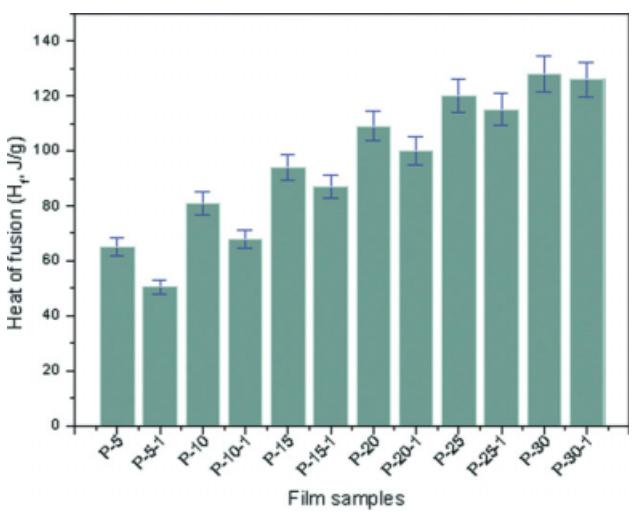

Figure 5 H_f values for P-5, P-10, P-15, P-20, P-25, and P-30 with and without glycerol. [Color figure can be viewed in the online issue, which is available at www.interscience.wiley.com.]

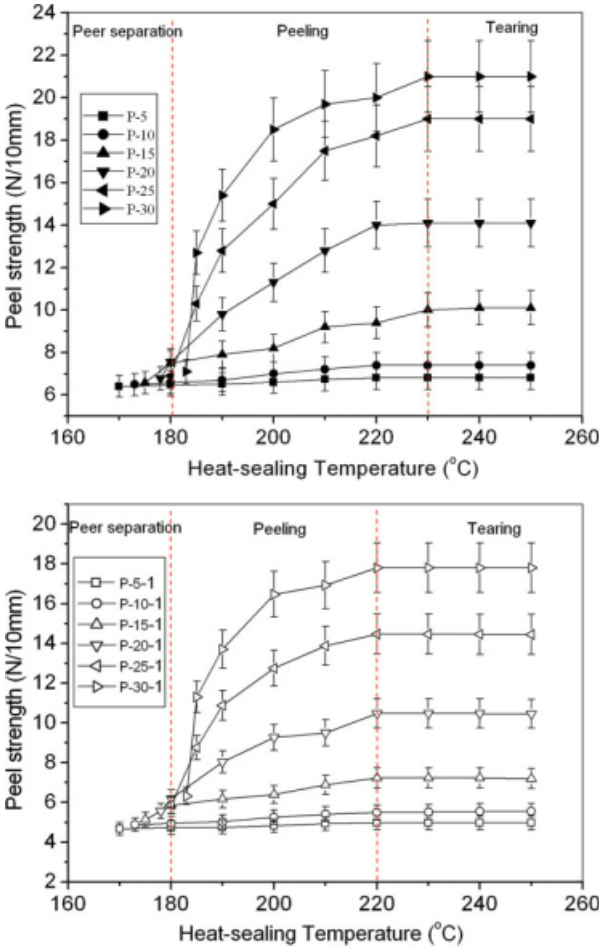

Figure 6 Effect of the heat-sealing temperature on the peel strength and failure types of the samples. [Color figure can be viewed in the online issue, which is available at www.interscience.wiley.com.]

two division temperatures of 180 and 230°C. This indicated that the molecules in laminated films were softened at a temperature of 180°C and adhered to each other in a state of conglutination; and then, the molecules inserted into and entangled with each other at a temperature of 230°C.

Another aspect taken into account was the influence of glycerol on the heat-sealing ability of the films. Plasticizers, such as glycerol and stearic acid, with lower molecular weights have been used to improve the flexibility and moisture resistance of natural films. These plasticizers are usually bound to the protein molecules via weak hydrogen bonds and leach out over time, affecting the mechanical properties of the films.[17,22] Therefore, it is necessary to evaluate the sealing results of the heat-sealing parts with the leached-out plasticizer. In others words, the heat-sealing parts should be recognized as new material to investigate the changes of its microstructure after heat sealing with prolonged time.[17] Only 1.0 wt % glycerol (on the basis of SPI) was mixed in samples P-5, P-10, P-15, P-20, P-25, and P-30 to determine the effect of glycerol on the peeling process. Similarly, each sample with glycerol also had three types of peeling results, separation, peeling, and tearing, in the temperature range 180–220°C. P-30-1 had the maximum increasing ratio of peel strength in the temperature range 180–220°C. Still, 180°C was the division temperature of the separation and peeling for all samples. However, the division temperature for the peeling and tearing processes decreased from 230 to 220°C. For the same content of SPI/PVA films, their tensile strength decreased with the addition of glycerol. This means that glycerol greatly affected the structure of the samples by decreasing the chain entanglement of the long molecules in the films. The mechanism of this phenomenon was that the existence of glycerol made it easy to move to the interface of the films and then prevent the contact of long molecules.[21,33]

Effect of the heat-sealing temperature on the tensile strength

Figure 7 shows the tensile strength of the heat-sealing samples (with/without glycerol) through circular

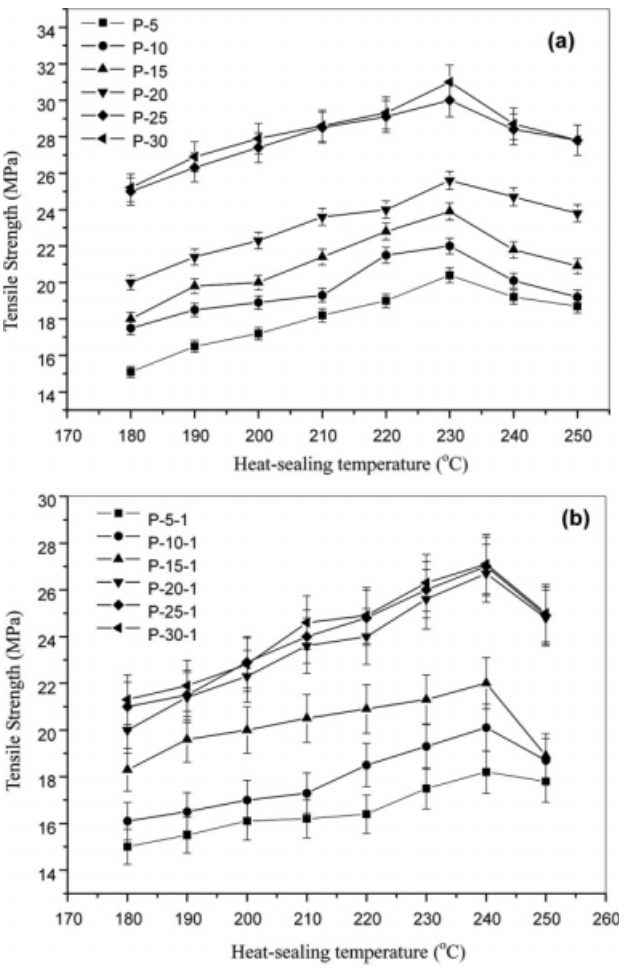

Figure 7 Relationship between the tensile strength and heat-sealing temperature for the samples with circle notches.

notch tensile tests (TD) under various heat-sealing temperatures. As it was confirmed that these samples had a phenomenon of peeling separation under 180°C, the heat-sealing temperature was set in the range of 180–250°C in this tensile strength test. In Figure 7(a), the tensile strength for all of the samples (P-5, P-10, P-15, P-20, P-25, and P-30) increased with increasing heat-sealing temperature and reached maximum values around 230°C and then decreased. This trend under 230°C was similar to that observed in the peel strength, which might have been an indication that adhesion between the films affected the mechanical strength of the heat-sealing area. The tensile strength increased with increasing adhesion strength between the films, and it got to the peak point when all of the blends were melted. With a higher PVA content in the film, the initial value of the tensile strength was higher at a heat-sealing temperature of 180°C. This result shows that the long molecule of PVA had a main function of resisting the stretching of the blends. Crystallization in blend was partly lost beyond a temperature of 230°C with the complete melting state. The higher the sealing temperature led to a greater quench-cooling effect with the result of fewer crystals and poorer tensile strength.[16] In another aspect, the molecules in the blend films may have been partly oriented during the film-casting process, which would have caused a high tensile strength in TD.[20,34] However, this orientation would have been disturbed under higher heat-sealing temperatures with complete melting. Therefore, the values of tensile strength for all of the samples decreased because of the previously mentioned two reasons.

The values of tensile strength for samples P-5-1, P-10-1, P-15-1, P-20-1, P-25-1, and P-30-1 are shown in Figure 7(b) to show the effect of the glycerol. With the addition of glycerol, the initial values of strength at 180°C had decreased for all samples. With increasing heat-sealing temperature, the strength increased for each film, similar to the sample without glycerol. The peak values of the tensile strength were obtained at a temperature of 240°C.

Crystalline structure as tested by XRD

As aforementioned, the peel strength was correlated to the microstructure of the interface structure of the laminated films, including the chain entanglement, orientation, and crystallization. So it is important to understand the effect of the heat-sealing temperature on the heat-sealing properties by characterization of the crystalline microstructure of the heat-sealing parts. Figure 8 shows the typical X-ray patterns of P-20 and P-20-1 before and after heat sealing at 220°C. The reason 220°C was selected as the heat-sealing temperature was that the samples were in a melting

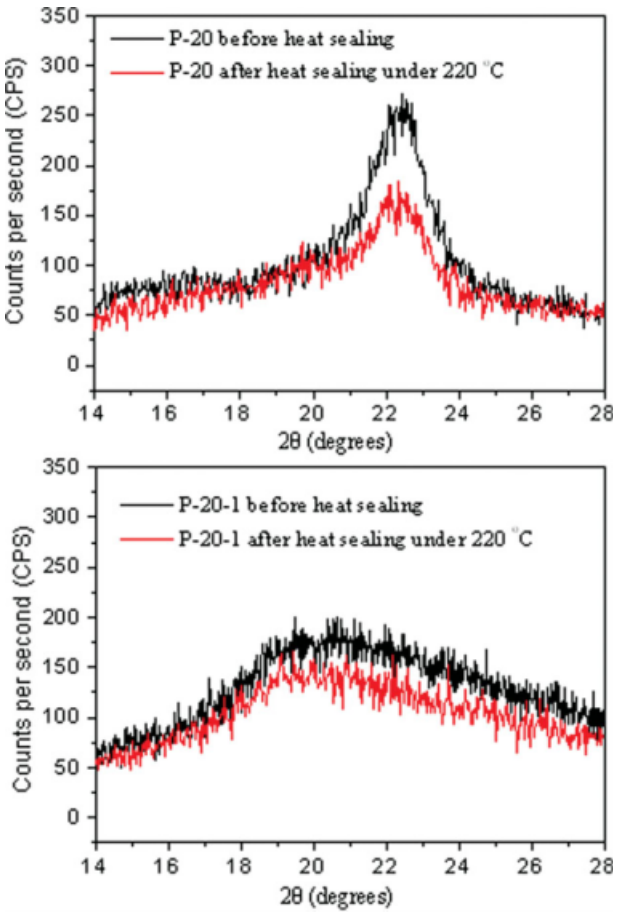

Figure 8 Typical XRD patterns of P-20 and P-20-1 before and after heat sealing at 220°C. [Color figure can be viewed in the online issue, which is available at www.interscience.wiley.com.]

and easy peeling state as the peel strength decreased. P-20 had an XRD peak at $2\theta = 22°$ in this test, which was similar to previous reported results.[21] After the heat-sealing process, the XRD peak (2θ) for P-20 did not shift; the intensity of the XRD peak was gentler than before. This indicated that the heat-sealing had greatly broken the crystalline structure of the blend and that the crystallization degree of the blend could not return to the original state, even with a short melting process.

The XRD peak of P-20-1 was about $2\theta = 20°$. It was seen ultimately that P-20-1 compatibilized by glycerol had an even less intense peak than P-20. This phenomenon must have been due to the breaking of the crystalline structure in PVA/SPI by small molecules. Glycerol was compatible with protein and could improve the mechanical properties of the films through decreasing intermolecular attraction and interfering with the protein packing. Moreover, glycerol limited the crystal growth of other polymers by interacting with these polymeric chains and hindering their alignment.[35]

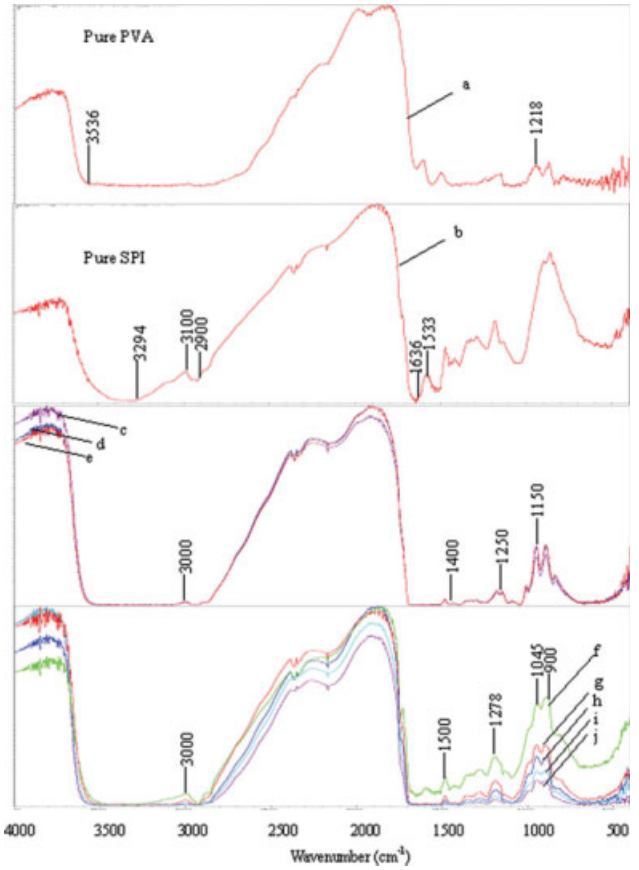

Figure 9 FTIR curves of the heat-sealing areas of samples at various temperatures: (a) pure PVA, (b) pure SPI, (c) P-20, (d) heat-sealing part of P-20 (180°C), (e) heat-sealing part of P-20 (220°C), (f) P-20-1, (g) heat-sealing part of P-20-1 (180°C), (h) heat-sealing part of P-20-1 (200°C), (i) heat-sealing part of P-20-1 (220°C), and (j) heat-sealing part of P-20-1 (240°C). [Color figure can be viewed in the online issue, which is available at www.interscience.wiley.com.]

Microstructure of the heat-sealing parts as tested with FTIR

Figure 9(a,b) show the FTIR curves of the pure PVA and SPI. The basic structure of the PVA molecule is —OH groups on carbon chains. At room temperature, the broad —OH absorption band was observed in the wave-number range 2918–3565 cm^{-1}. The absorption at 3294 cm^{-1} in SPI referred to the hydrogen-bond association between the protein chains and moisture in the protein. There was obvious absorption of the —NH— band in the ranges 1636–1680 and 1533–1559 cm^{-1}. These bands accorded with the reported soy protein spectrum with an amide I band at 1632 cm^{-1} and an amide II band at 1536 cm^{-1}.[22]

As shown in Figure 9(c), the FTIR spectra of P-20 had absorption bands at 1636–1533 and 1150–1250 cm^{-1} because of —NH—, C—N stretching and N—H bending (amide III) vibrations, respectively. A typical characterization of these spectra was the disappearance of the strong hydrogen-bond association, which both appeared in the SPI and PVA spectra, where a new absorption band at 2900–3100 cm^{-1} appeared. These band-shifts suggest that there is a specific chemical interaction occurring between SPI and PVA. The new band may have referred to the hydrogen-bond association between the protein chains and PVA. After heat-sealing at temperatures of 180 and 230°C, the FTIR spectra of P-20 shown in Figure 9(d,e) nearly totally overlapped with each other, which means that the heat-sealing process nearly did not affect the band structure of the blends.

Figure 9(f–j) shows the FTIR spectra of P-20-1 and its heat-sealing parts (180, 200, 220, and 240°C). By comparing the FTIR curves of P-20 and P-20-1, we determined that glycerol (1.0 wt % of SPI) did not greatly change the main FTIR bands. Meanwhile, the IR absorbances of the SPI/PVA/glycerol depended on the heat-sealing temperatures. The absorption intensity of the 1000-, 1200-, and 1500-cm^{-1} bands obviously decreased with increasing heat-sealing temperature from 180 to 240°C. Compared to the spectra of SPI and PVA, the five peaks at 850, 900, and 1045 cm^{-1} (C—O stretching at C^1 and C^3) and 1117 cm^{-1} (C—O stretch at C^2) were clearly observed only for the SPI resin with glycerol. This indicates that at least some glycerol molecules were present in the free form in the cured SPI resin.[36] The presence of glycerol also decreased the absorption because of the stretching of the carbonyl peak in primary amide at 1641 cm^{-1}; this indicated lesser amide bonds. However, these bands formed with the glycerol were easily broken through molecule thermal liberation. These variations may be attributed to the leaching of water and glycerol from the blend films during the heat-sealing process.[37]

Morphology of the heat-sealing areas

Morphological analysis helped us to clearly determine the conditions of the heat-sealing area. Optical microscopy, infrared microspectroscopy, and SEM were applied to observe the interface changes in the laminated films.[16,37,38] Figure 10(a–c) show the optical photographs of the pure SPI, P-5, and P-5-1 films in a rolling state with a size about of 50 × 50 cm^2; these were large enough for mechanical property characterization. As shown in Figure 10(d), P-20-1 was in an expanding state with good properties of integrality, transparence, and flexibility. Figure 11 shows the SEM morphology details of the heat-sealing films at various temperatures. The separation surface of P-20 at 180°C is shown in Figure 11(a). The two black arrows point to the directions of peel strength. A separation line of laminated films was clearly observed in the upside of this figure. As the interfacial strength mainly depended on the number

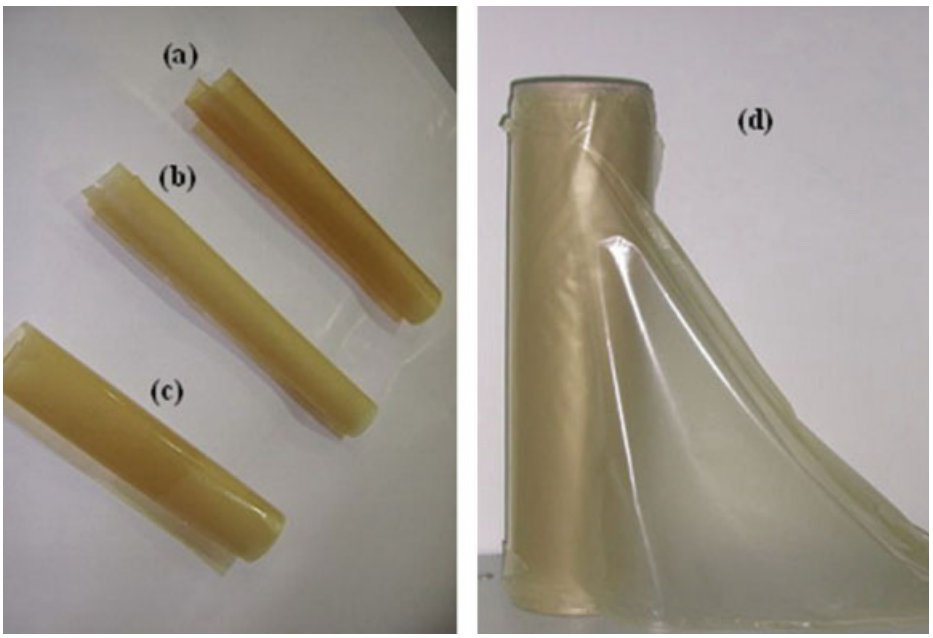

Figure 10 Photographs of the SPI/PVA blend films: (a) the pure SPI film, (b) P-5, (c) P-5-1, and (d) P-20-1. [Color figure can be viewed in the online issue, which is available at www.interscience.wiley.com.]

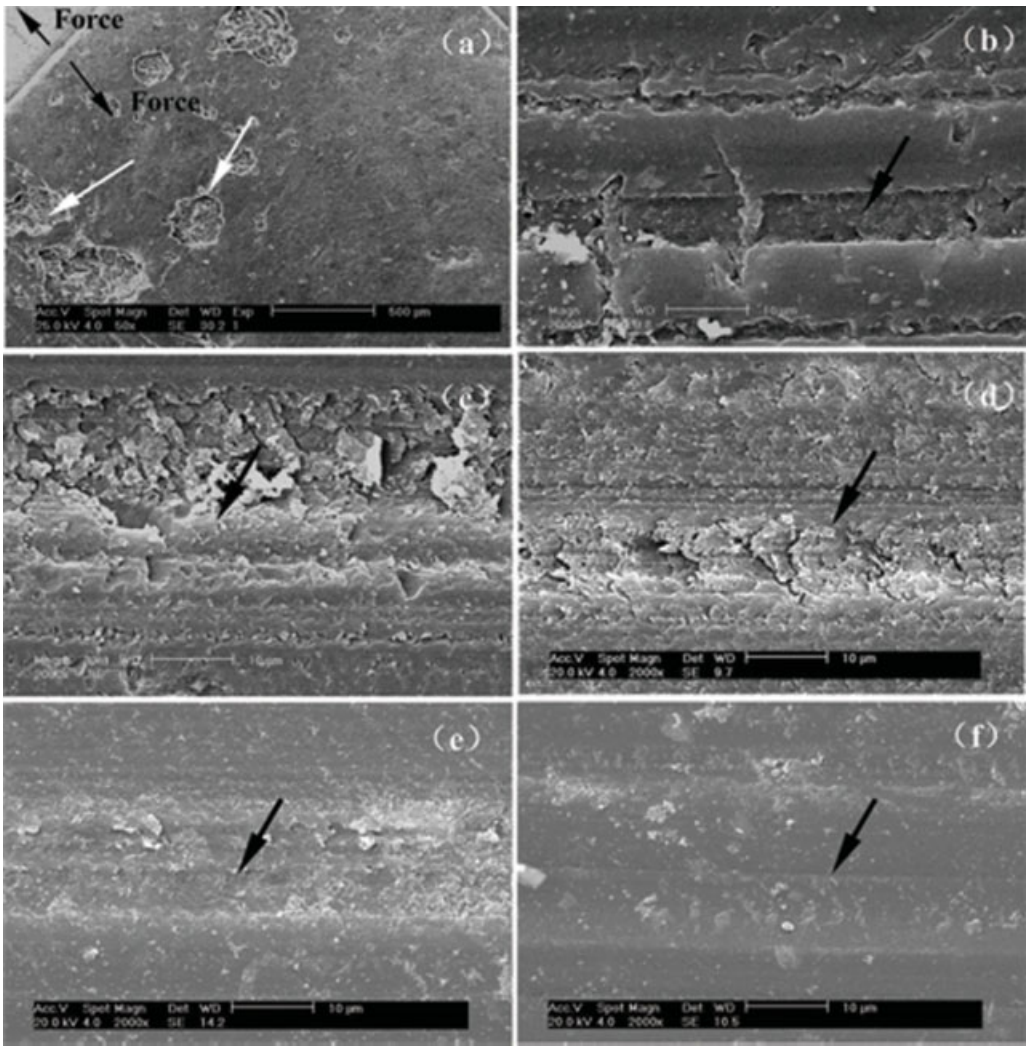

Figure 11 SEM morphology of the heat-sealing areas: (a) the separation surface of heat-sealing P-20 between the two layers in contact; (b–e) the cross-section morphology of P-20 after heat sealing at 220, 230, 240, and 250°C, respectively; and (f) the cross-section morphology of P-20-1 after heat sealing at 240°C.

of entangled chains forming connections across the interface, the easy separation indicated that the molecules of P-20 could not yield more entanglement at a lower temperature of 180°C. Although the heat-sealing properties were not satisfied, the interfaces of the laminated films still were broken by peel force. In the peeling process, some areas of the film were ripped off, which was attributed to the adhesive capacity of the laminated films.

Figure 11(b–e) shows the cross-sectional morphologies of P-20 after heat sealing at temperatures of 220, 230, 240, and 250°C, respectively. With increasing temperature, the laminated films merged into each other at different degrees. In Figure 11(b), melting and diffusing areas, pointed by an arrow, indicated that the molecules had formed connections and across the interface. Higher temperature accelerated the molecular movement in the interface. At 250°C, as shown in Figure 11(e), sufficient fusion made the interface of P-20 disappear. This indicated that only at the temperature at which these chains melted and diffused across the interface could a high adhesive capacity be realized. The higher adhesive capacity led to higher peel strength because of the chain entanglements. Figure 11(f) shows the cross-sectional morphologies of P-20-1 after heat sealing at a temperature of 240°C. With the addition of glycerol, the laminated films also completely fused, which led to a satisfying development of peeling strength. Through these observations, we found the heat-sealing temperatures (set temperatures) were higher than those given by DSC. This phenomenon was attributed to the thermal barrier of the polymeric materials, which has been reported before.[39,40]

CONCLUSIONS

The heat-sealing properties of PVA/SPI films with/without compatibilization by glycerol were investigated. The SPI/PVA blend films were found to hold superior heat-sealing abilities to pure SPI films. Also, the PVA and glycerol contents in the blend films and the temperature were main factors controlling the mechanical properties of the films. Moreover, the heat-sealing temperature of the films greatly affected their crystalline structure. After a short melting time, the blend crystallization degree could not convert to the original state in a short cooling time. The long-chain molecules of PVA blended with SPI caused entanglement and intermolecular hydrogen bonding, which enhanced T_m and H_f of the films. Glycerol destroyed the crystalline microstructure, and the SPI/PVA blends needed less heat to be converted to the melting state. We confirmed by SEM that the heat-sealing process was a process of chains melting and diffusing through the laminated interface, which strongly depended on the temperature: a higher temperature led to a higher adhesiveness and a higher peel strength because of the chain entanglements.

References

1. Zhou, Z.; Zheng, H.; Wei, M.; Huang, J.; Chen, Y. J Appl Polym Sci 2008, 107, 3267.
2. Ralston, B. E.; Osswald, T. A. Plast Eng 2008, 64, 36.
3. Wang, N. G.; Zhang, L. Polym Int 2005, 54, 233.
4. Swain, S. N.; Rao, K. K.; Nayak, P. L. Polym Int 2005, 54, 739.
5. Nayak, P.; Sasmal, A.; Nanda, P. K.; Nayak, P. L.; Kim, J.; Chang, Y. W. Polym Plast Technol Eng 2008, 47, 466.
6. Ahmed, J.; Ramaswamy, H. S.; Raghavan, G. S. V. LWT Food Sci Technol 2008, 41, 71.
7. Zheng, H.; Zhou, Z. Y.; Chen, Y.; Huang, J.; Xiong, F. L. J Appl Polym Sci 2007, 106, 1034.
8. Yu, J. H.; Cui, G. J.; Wei, M.; Huang, J. J Appl Polym Sci 2007, 104, 3367.
9. Skorepova, J.; Moresoli, C. J Agric Food Chem 2007, 55, 5645.
10. Hernandez-Izquierdo, V. M.; Krochta, J. M. J Food Sci 2008, 73, R30.
11. Kumar, R.; Liu, D.; Zhang, L. J Biobased Mater Bioenergy 2008, 2, 1.
12. Rhim, J. W.; Lee, J. H.; Ng, P. K. W. LWT Food Sci Technol 2007, 40, 232.
13. Sothornvit, R.; Olsen, C. W.; Mchugh, T. H.; Krochta, J. M. J Food Eng 2007, 78, 855.
14. Choi, W. Y.; Lee, C. M.; Park, H. J. LWT Food Sci Technol 2006, 39, 591.
15. Yuan, C. S.; Hassan, A.; Ghazali, M. I. H.; Ismail, A. F. J Appl Polym Sci 2007, 104, 3736.
16. Hashimoto, Y.; Ishiaku, U. S.; Leong, Y. W.; Hamada, H.; Tsujii, T. Polym Eng Sci 2006, 46, 205.
17. Aithani, D.; Lockhart, H.; Auras, R.; Tanprasert, K. J Plast Film Sheeting 2006, 22, 247.
18. Halim, L.; Pascall, M. A.; Lee, J.; Finnigan, B. J Food Sci 2009, 74, 9.
19. Chukhlanov, V. Y.; Tereshina, E. N. Polym Sci Ser C 2007, 49, 288.
20. Poisson, C.; Hervais, V.; Lacrampe, M. F.; Krawczak, P. J Appl Polym Sci 2006, 99, 974.
21. Su, J. F.; Huang, Z.; Liu, K.; Fu, L. L.; Liu, H. R. Polym Bull 2007, 58, 913.
22. Su, J. F.; Huang, Z.; Yang, C. M.; Yuan, X. Y. J Appl Polym Sci 2008, 110, 3706.
23. Ahmed, J.; Ramaswamy, H. S.; Raghavan, G. S. V. LWT Food Sci Technol 2008, 41, 71.
24. Tsujii, T.; Ishiaku, U. S.; Kitagawa, K.; Hashimoto, Y.; Mizoguchi, M.; Hamada, H. Plast Rubber Compos 2005, 34, 189.
25. Tetsuya, T.; Ishiaku, U. S.; Mizoguchi, M.; Hamada, H. J Appl Polym Sci 2005, 97, 753.
26. Kurose, T.; Urman, K.; Otaigbe, J. U.; Lochhead, R. Y.; Thames, S. F. Polym Eng Sci 2007, 47, 374.
27. Abd El-Kader, F. H.; Shehap, A. M.; Abo-Ellil, M. S.; Mohmoud, K. H. J Appl Polym Sci 2005, 95, 1342.
28. Adoor, S. G.; Manjeshwar, L. S.; Naidu, B. V. K.; Sairam, M.; Aminabhavi, T. A. J Membr Sci 2006, 280, 594.
29. Kubo, S.; Kadla, J. F. Biomacromolecules 2003, 4, 561.
30. Sudhamani, S. R.; Prasad, M. S.; Sankar, K. U. Food Hydrocolloids 2003, 17, 245.

31. Jo, C.; Kang, H. J.; Lee, N. Y.; Kim, Y. J.; Byun, M. W. Food Sci Biotechnol 2004, 13, 712.
32. Wang, Y. X.; Cao, X. D.; Zhang, L. N. Macromol Biosci 2006, 6, 524.
33. Lu, Y. S.; Weng, L. H.; Zhang, L. N. Biomacromolecules 2004, 5, 1046.
34. Raj, B.; Jagadish, R. S.; Srinivas, P.; Siddaramaiah.J Appl Polym Sci 2005, 96, 1193.
35. Ma, X. F.; Yu, J. G.; He, K. Macromol Mater Eng 2006, 291, 1407.
36. Preeti, L.; Anil, N. N. Ind Crops Prod 2005, 21, 49.
37. Lodha, P.; Netravali, A. N. Ind Crops Prod 2005, 21, 49.
38. Cho, S. W.; Usten, H.; Galstedt, M.; Hedenqvist, M. S. J Biobased Mater Bioenergy 2007, 1, 56.
39. Tetsuya, T.; Hashimoto, Y.; Ishiaku, U. S.; Mizoguchi, M.; Leong, Y. W.; Hamada, H. J Appl Polym Sci 2006, 99, 513.
40. Mueller, C.; Capaccio, G.; Hiltner, A.; Baer, E. J Appl Polym Sci 1998, 70, 2021.